EurJOC
European Journal of Organic Chemistry

Full Papers
doi.org/10.1002/ejoc.202100022

Chemistry Europe
European Chemical Societies Publishing

Special Collection

Stereoselective Organocatalytic Construction of Spiro Oxindole Pyrrolidines Using Unsaturated α-Ketoesters and α-Ketoamides

Tibor Peňaška,[a] Vitalii Palchykov,[a, b] Erik Rakovský,[c] Gabriela Addová,[a] and Radovan Šebesta*[a]

We have investigated the stereoselective formation of spiro oxindole pyrrolidines via formal [3+2] cycloaddition of oxindole imines with ketoesters and ketoamides. Bifunctional squaramide organocatalyst was able to induce enantioselectivity of up to 60% ee, increased to 72% ee after re-crystallization, in the formation of spiro pyrrolidines with ketoesters. Interestingly, ketoamides provided alternative spiro oxindole pyrrole products in addition to the main product, which was formed via a different reaction pathway. Structures of spiro oxindole pyrrolidine as well as pyrrole products were confirmed by X-ray crystallographic analysis. Two new squaramide based catalysts were synthesized and tested. DFT calculation helped elucidate the reaction course.

Introduction

Carbo- and heterocyclic structures are omnipresent in natural products and human-made drugs, and other bioactive compounds. Many synthetic methods are devoted to the construction and manipulation of heterocyclic compounds. However, efficient synthesis and functionalization of chiral heterocycles have been identified as persisting synthetic challenges from the pharmaceutical industry's standpoint.[1]

The significance of chiral heterocycles has been recognized as an important task, and various catalytic methods are being developed both by transition metal catalysis,[2] and organocatalysis.[3] Indol-based chiral heterocycles,[4] and more specifically, those with oxindole core are prominent core structures among bioactive heterocyclic compounds. Because of their wide-spread occurrence and importance, many synthetic strategies have been devised for their preparation.[5] Spirooxindol core is an interesting structural motif found in natural alkaloids, such as horsfiline, rychnophylline, or spirotryprostatins, and several pharmaceuticals with anticancer or antiviral properties.[6] Organocatalytic strategies towards spirooxindols utilize a variety of activation modes. Initially, covalent enamine/iminium activation led to spirooxindols with fused six-membered rings.[7] Later, activation modes based on non-covalent interactions also led to many strategies towards various chiral spirooxindol derivatives. Spirooxindol pyrrolidines were synthesized by [3+2]-type cycloadditions, which rely mostly on non-covalent activation by chiral Brønsted acids or hydrogen bond donors such as thioureas or squaramides. The typical strategy involves [3+2] cycloaddition of isatin-derived azomethine ylides with activated alkenes. Again, enones and α,β-unsaturated aldehydes benefit from iminium activation.[8] Xu and co-workers developed squaramide-catalyzed asymmetric dipolar cycloaddition between azomethine ylide and aromatic nitroalkenes.[9] Azomethine ylide was formed *in situ* from an imine via a 1,3-proton shift. Based on this strategy, fluorinated imines reacted with nitroalkenes too.[10] Isatine-derived azomethine ylides underwent dipolar cycloaddition with arylidene azlactones or maleimides when chiral thioureas or squaramides were used as catalysts.[11] Other, somewhat less reactive dipolarophiles, such as activated alkynes, allenes, methyleneindolinones, or imines, required stronger Brønsted acid for activation.[12] Oxindol-core was recently incorporated into axially-chiral compounds via atroposelective kinetic resolution mediated by Brønsted acids.[13]

As a part of our interest in the organocatalytic formation of chiral heterocycles, we have recently investigated [3+2] cycloaddition of azomethine ylides with unsaturated esters.[14] In this work, we have found out that unsaturated esters probably bind inefficiently to various hydrogen-bonding organocatalysts, which led to a racemic reaction. We reasoned that analogous unsaturated ketoesters or ketoamides might be much more efficient acceptors of hydrogen bonds from a chiral catalyst. This fact could lead to an enantioselective dipolar cycloaddition reaction. In this context, we decided to study the formal cycloaddition of azomethine ylides generated from oxindole imines and unsaturated keto esters and keto amides. Herein, we

[a] Dr. T. Peňaška, Dr. V. Palchykov, Dr. G. Addová, Prof. Dr. R. Šebesta
Department of Organic Chemistry, Faculty of Natural Sciences,
Comenius University in Bratislava
Mlynská dolina, Ilkovičova 6, 84215 Bratislava, Slovakia
E-mail: radovan.sebesta@uniba.sk
www.radovansebesta.com
[b] Dr. V. Palchykov
Research Institute of Chemistry and Geology
Oles Honchar Dnipro National University
Gagarina Av. 72, Dnipro, 49010, Ukraine
[c] Dr. E. Rakovský
Department of Inorganic Chemistry
Faculty of Natural Sciences, Comenius University in Bratislava
Mlynská dolina, Ilkovičova 6, 84215 Bratislava, Slovakia

Supporting information for this article is available on the WWW under https://doi.org/10.1002/ejoc.202100022

Special Collection Part of the "Organocatalysis" Special Collection.

present results of the investigation of organocatalyzed formal dipolar cycloaddition of imine-derived azomethine ylides with unsaturated ketoesters and amides.

Results and Discussion

We started our study with testing of several quinine-based organocatalysts **C1**-**9** in a model multicomponent reaction system. The reaction between *N*-benzylisatine (**1a**), benzylamine (**2**), and β,γ-unsaturated α-ketoester **3a** afforded spirooxindole pyrrolidine **4a** with four stereogenic centers adjacent (Scheme 1).

In our previous study, bifunctional quinine-based squaramides afforded racemic but diastereomerically pure cycloaddition products with unsaturated esters.[14] With ketoester **3a**, we assumed a better activation via hydrogen bonds due to the presence of two carbonyl groups. More efficient catalyst-substrate binding could result in higher stereoselectivity too. Reactions were performed in dichloromethane (DCM) for 1–24 h with 10 mol-% of catalyst. It was crucial to mix first benzylisatine (**1a**) with benzylamine (**2**) and stir for a few minutes at −5 °C and only then add the keto ester **3a**. This addition order was necessary for preventing undesired competitive reaction between benzylamine (**2**) and ketoester **3a**. We also observed partial decomposition of imine intermediate after one hour. Therefore, the reaction is started at a lower temperature of −5 °C. Using squaramide catalyst **C1**,[15] we obtained new spirocyclic oxindole **4a** in a good yield (73%) but with low enantiomeric purity of 18% ee. Lowering the temperature to −30 °C and longer reaction time led only to a small improvement of selectivity with catalyst **C1** (34% ee). The squaramide catalyst **C2**[16] gave a slightly lower yield (57%) but considerably higher enantioselectivity (60% ee). The lower temperature did not improve the selectivity with catalyst **C2**. Diastereoisomeric, quinidine-based catalysts **C3**, and **C4** were also tested.[15–16] This little difference of spatial arrangement caused decrease of selectivity and yield (46–64%, 12–26% ee). We have synthesized new squaramide catalysts **C5** and **C6**, which have phenyl group on the double bond of the quinuclidine moiety. The phenyl group has been installed by a Pd-catalyzed Heck reaction with phenyl bromide (for more details, see SI). We hypothesized that additional π-π stacking between reactants and catalyst might improve selectivity. However, no improvement of reaction outcomes was observed.

Product **4a** was obtained in yield 52–57% and selectivity 23–42% ee. The catalyst **C6** with a longer carbon chain provided higher selectivity than catalyst **C5**. When catalyst **C7** with two quinine units was used,[17] the chemical yield of the product was 60%, and enantiomeric excess was 20% ee. In comparison with squaramides, thioureas typically have lower acidity and different distance of hydrogen bond donor sites. There was no significant change in yield (60%) and enantioselectivity (20% ee) with thiourea catalyst **C8**.[18] Commercially available natural quinine (**C9**) gave product **4a** in low yield (26%) as a racemate. The results of the initial catalyst screening in terms of yields and enantioselectivity are summarized in Figure 1.

We continued our investigation by screening several other hydrogen-bond donor catalysts in the reaction of isatine **1a**, benzylamine (**2**), and ketoester **3a** (Figure 2). The results show that squaramides with tertiary (**C10** and **C11**),[19] secondary (**C12**)[20] and primary (**C13**)[19a] amino group gave the required product **4a** with moderate yield (28–53%) and very poor enantiomeric purities (4–16% ee). Aminoindanol squaramide **C14**[21] with a free hydroxyl group afforded comparable results. Thiosquaramides, as sulfur derivatives of commonly used squaramides, have been studied in recent years due to their higher acidity compared to squaramides. When we carried out the model reaction with thiosquaramides **C15**, and **C16**,[22] the cycloaddition product **4a** was obtained in good yields (46–77%) but in virtually racemic form. Various other catalysts, such

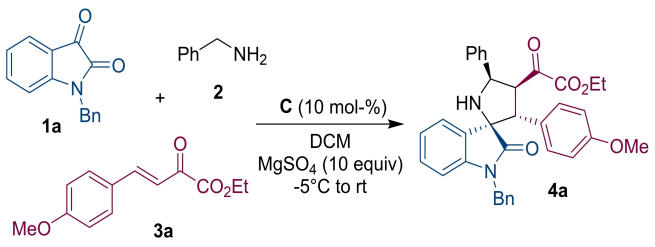

Scheme 1. Test multicomponent reaction for the screening of catalysts.

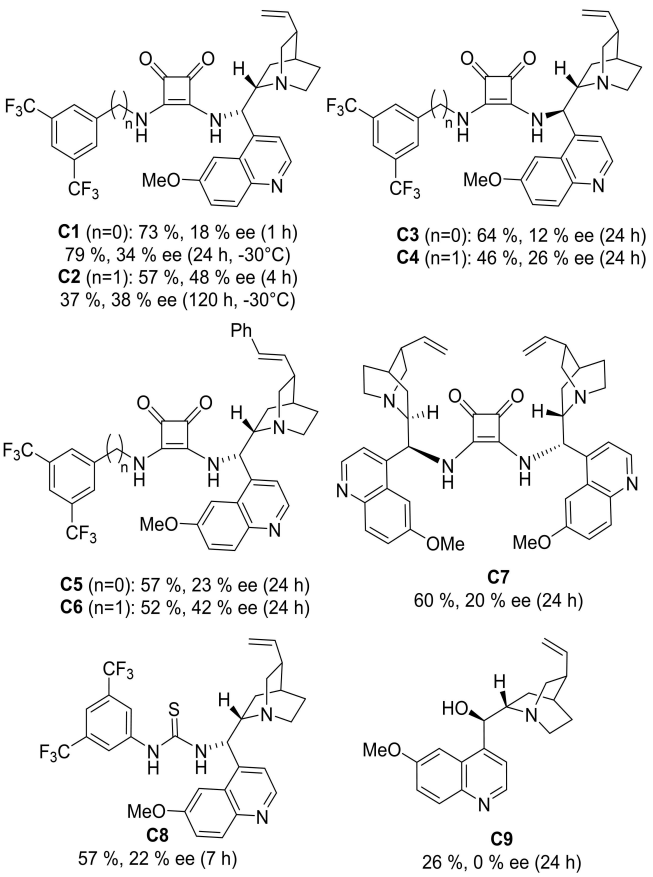

Figure 1. Quinine-based catalysts used in this study.

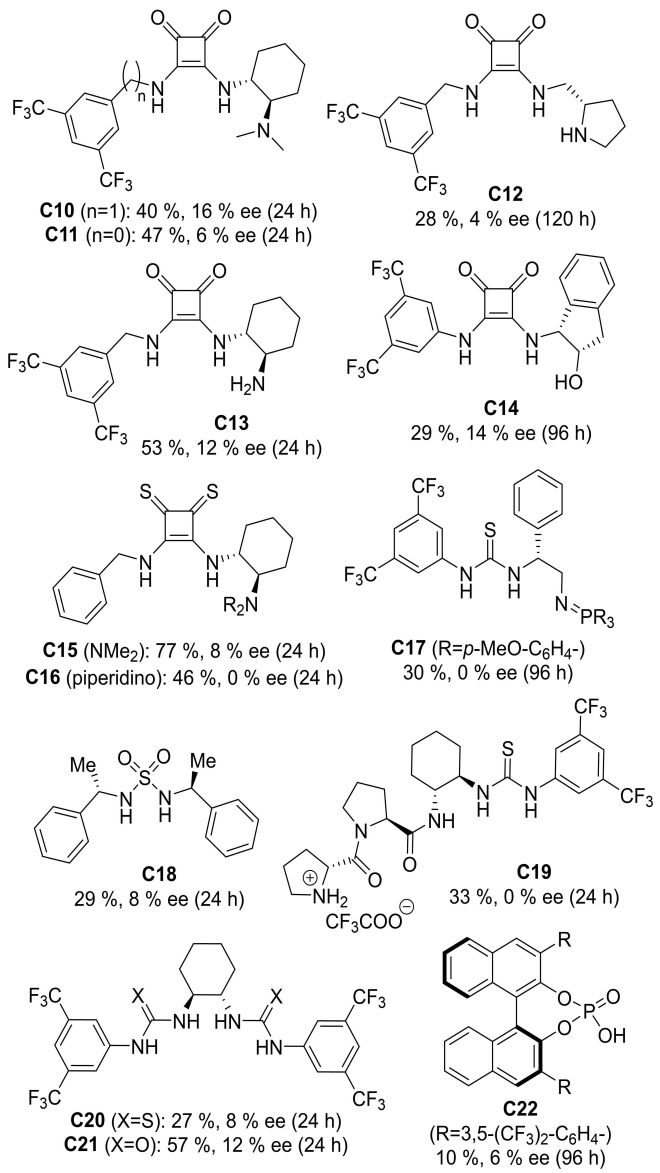

Figure 2. Other catalysts used in this study.

as Dixon's thiourea **C17**[23] with a strongly basic center, sulfamide catalyst **C18**,[24] hybrid peptide-thiourea **C19**, thio/ureas **C20**,[25] and **C21**[26] and also commercially available chiral phosphoric acid **C22**[27] gave the product **4a** in moderate yield (10–57%) and with very low enantioselectivity (0–12% ee).

The reaction did not proceed when guanidines (**C23** and **C24**) and phase-transfer catalysts (**C25** and **C26**) were used, for catalyst structures, see SI. For more details of the testing conditions and preparation of racemic samples for HPLC analysis, see SI.

We selected the most efficient catalyst, quinine-based squaramide **C2**, that gave the best enantioselectivity (60% ee) for further optimization.

First, we have studied the effect of solvent on the cycloaddition of benzylisatin (**1a**), benzylamine (**2**) and keto ester **3a**. We have employed standard conditions (rt, 24 h) with 10 mol% of organocatalyst **C2**. As mentioned above, the reaction in dichloromethane proceeded with the yield of 57% and the enantiomeric excess 60% ee (Table 1, entry 1). Other tested chlorinated solvents, 1,2-dichloroethane (DCE), and $CHCl_3$ gave slightly lower yields and enantioselectivity (Table 2, entries 2–3). In cyclic ethers such as THF, 2-methyltetrahydrofuran (Me-THF), and 1,4-dioxane, the reaction had the highest enantioselectivity of 60% ee, but yields were lower than in DCM (Table 1, entries 4–6). Surprisingly, a mixture of DCM and 1,4-dioxane (v/v 1:1) brought a lower enantioselectivity 44% ee of the cycloaddition (Table 1, entry 7). Slightly lower yields and enantioselectivities were observed in acyclic ethers compared to cyclic ones (Table 1, entries 8–10). The cycloaddition also proceeded in aromatic solvents toluene, xylene, and trifluoromethylbenzene (Table 1, entries 11–13), but neither yield nor enantioselectivity was improved. Solvents with a free hydroxy group (2,2,2-trifluroethanol, methanol, and L-ethyl lactate) were not suitable for this reaction. In these solvents, the reactions did not proceed, and only starting materials were recovered. Protic solvents probably hindered the formation of the azomethine ylide, thus making the cycloaddition ineffective.

In the further inquiry, we focused on the effect of additives (Table 2). Acidic additives, such as benzoic and *p*-nitrobenzoic acid, caused a decrease in yield and stereoselectivity (Table 2, entries 2–3). On the other hand, a base diisopropylethylamine (DIPEA) and dimethylacetamide (DEA) as an additive solvent for higher solubility, gave comparable result as the reaction without any additives (Table 2, entries 1 and 4–6). Re-crystallization of the spiro-oxindol product **4a** from absolute ethanol increased its enantiomeric purity up to 72% ee (Table 2, entries 1 and 5, see in brackets).

We have evaluated the [3+2] cycloaddition reaction scope using a set of ketoesters **3a–f** with squaramide catalyst **C2**. In general, as shown in Table 3, keto esters **3a–d** with an electron-donating substituent on the aromatic core provide better results than those with electron-withdrawing substituents **3e–f** (Table 3, entries 1–4 *vs.* entries 5–6). On the other hand, the substituent R^1 on the ester functional group affects hydrogen-bond activation, thus on yield and selectivity. The best enantioselectivity (48–52% ee) was obtained using ethyl ester **3a** and *tert*-butyl ester **3d** (Table 1, entries 1 and 4) compared with benzyl ester **3b** and methyl ester **3c** (Table 1, entries 2–3). We have assumed that this is due to the steric effect and possible competitive π-π bonding of benzene core between the ester functional group and other aromatic systems in the reaction mixture. We examined the activity of catalyst **C1** with substrates **3a–b**. The corresponding products **4a–b** were isolated in higher yields but with markedly lower selectivity than with catalyst **C2** (Table 1, entries 1–2, see in brackets). Lowering the temperature to −30 °C did not provide better results (Table 1, entry 4).

We have briefly explored the use of *N*-methylisatine in this type of cycloaddition. However, the related products were probably unstable and challenging to analyze by chiral HPLC, see SI for characterization data.

Next, we turn our attention on α,β-unsaturated keto amides **5a–d**, which were easily prepared from the appropriate (*E*)-4-(4-

Table 1. Solvent screening in the reaction between oxindole **1a**, benzylamine (**2**) and ketoester **3a**.

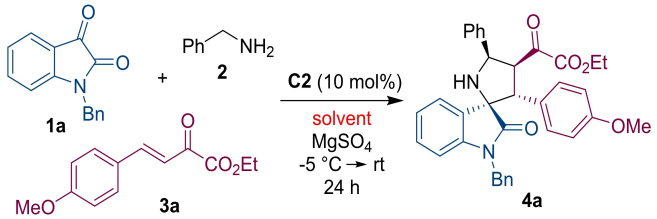

Entry	Solvent	Yield **4a** [%]	ee [%]
1	DCM	57 (73)[a]	60 (18)[a]
2	DCE	47	43
3	$CHCl_3$	56	32
4	THF	34	60
5	Me-THF	42 (40)[a]	60 (18)[a]
6	1,4-dioxane	26 (40)[a]	60 (20)[a]
7	1,4-dioxane/DCM (1:1)	36	44
8	TBME	29	44
9	CpOMe	33	54
10	DME	29	54
11	Toluene	37	30
12	Xylene	21	26
13	Ph-CF_3	54	48
14	CF_3CH_2OH	0	–
15	MeOH	0	–
16	L-ethyl lactate	0	–

[a] Data in brackets are for catalyst **C1** (10 mol%).

Table 2. Additive effects on the cycloaddition of benzylisatine (**1a**), benzylamine (**2**) and ketoester **3a**.

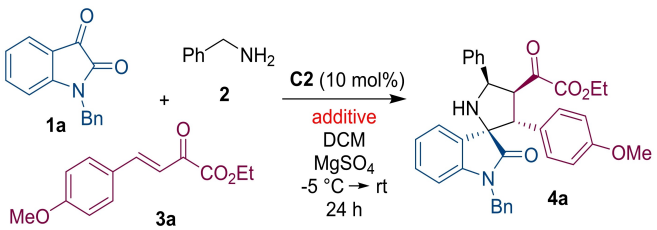

Entry	Additive (equiv)	Yield [%]	ee [%]
1	–	57	60 (72)[b]
2	*p*-Nitrobenzoic acid (2 equiv)	10	0
3	Benzoic acid (0.5 equiv)	36	26
4	DIPEA (0.5 equiv)	49	58
5[a]	DIPEA (0.5 equiv)	47	57 (67)[b]
6	Dimethylacetamide (1 equiv)	33	55

[a] Reaction in Me-THF/DCM (2:1). [b] Data in brackets are enantiomeric excess of product **4a** after re-crystallization in abs. EtOH at 5 °C.

methoxyphenyl)-2-oxobut-3-enoyl chloride (see SI). We tested these keto amides with quinine-based catalyst **C2** that gave good results with ketoesters **3**. These reactions provided corresponding spiro-oxindole pyrrolidines **6** with keto amide substituents. Spiro-oxindole pyrrolidines **6** were formed as a mixture of three diastereoisomers in a typical ratio of d.r. 4:3:2. These diastereomers were separated by column chromatography. Interestingly, a new unexpected spiro-oxindole **7** was formed with ketoamides **5a–c** (Scheme 2). The results are summarized in Table 4. Products **6** were isolated in moderate yields of 20–68% with low enantiomeric purities of 0–18% ee. For more details (reaction with catalyst **C1** see SI.

In addition to 1D and 2D NMR spectroscopy, structures, and configurations of products **4a**, **6a**, **6b**, and **7a** were unambiguously determined by single-crystal X-ray diffraction analyses (Figure 3). For details, see SI.

From a mechanistic point of view, these results can be explained by the formation of enolate **A** as a key intermediate. On the one hand, enolate **A** predictably converts into spirocycle **B**, which upon protonation affords main spirocyclic products **6** (Scheme 3, *route I*). The chemoselectivity of this step depends explicitly on the nature of the amide group. The content of the side product **7** is larger for dialkylamino groups NMe_2 and $N(CH_2)_4$. On the other hand, pyrrole products **7** were not observed with monoalkylamino group NHMe and NHBn. Unfortunately, the enantiomeric purity of all products was low (up to 26% ee).

Table 3. Functional group effect-keto esters.

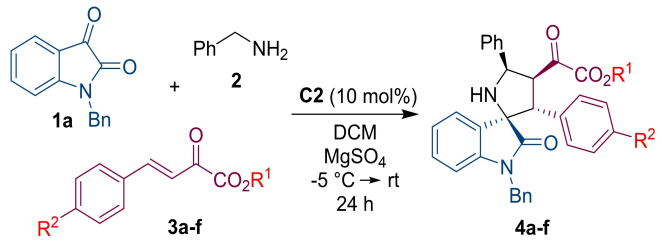

Entry[a]	R^1	$R^{2[b]}$	Product	Yield [%]	ee [%]
1	Et	MeO	**4a**	57 (73)[a]	60 (18)[a]
2	Bn	MeO	**4b**	43 (72)[a]	30 (0)[a]
3	Me	MeO	**4c**	71	28
4	*t*Bu	MeO	**4d**	87 (78)[b]	52 (48)[b]
5	Et	Br	**4e**	35	nd[c]
6	Bn	Br	**4f**	27	nd[c]

[a] Data in brackets are for catalyst **C1** (10 mol%). [b] Data in brackets are for the reaction at −30 °C. [c] Optimal conditions for HPLC were not found.

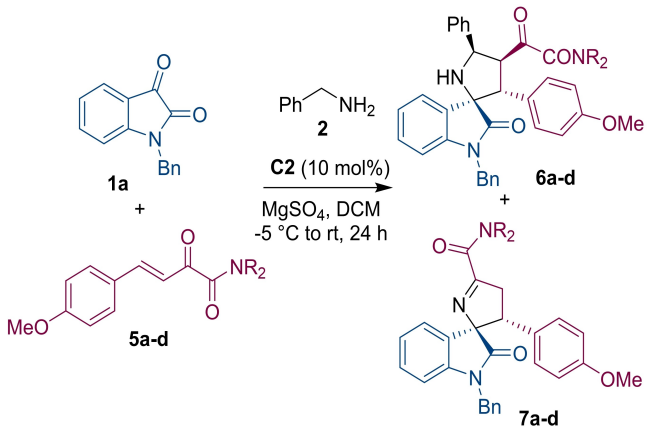

Scheme 2. [3 + 2] cycloaddition reaction with keto amides **5**.

On the other hand, enolate **A** can be protonated by a conjugate base formed in previous steps (Scheme 3, *route II*). In this way, formed intermediate **C** can undergo cyclization via the addition of imine nitrogen atom on the keto amide carbonyl to produce intermediate **D**, which can then form 1,3-oxazetidine **E**. Alternatively, the formation of intermediate **E** can proceed directly from intermediate **C** as a [2 + 2]-type cycloaddition. After the elimination of benzaldehyde, final product **7** is formed. GCMS and ^{1}H NMR confirmed the presence of benzaldehyde in the reaction mixture. Structures, absolute and relative configurations of compounds **6** and **7** were confirmed by NOESY spectroscopy and X-ray crystallographic analysis (see SI). The reason ketoamides also undergo a secondary pathway towards pyrrole products **7** might be explained by the higher basicity of the ketoamide enolate **A** compared to corresponding ketoester enolate. It is due to the stronger electron-withdrawing effect of the ester group in comparison with an amide. Therefore, protonation of the more basic ketoamide enolate (*route II*) thus competes with the main reaction *route I* towards spiro-oxindol pyrrolidines **4** and **6**. The differences between ketoester and ketoamide enolates likely also influence the diastereoselectivity of the reaction. Protonation/deprotonation of these enolates can change enolate configuration and thus may lead to different facial preferences in the ring-closing step of the reaction (see Supporting information for more details).

To understand the mechanisms of the formation of spirocyclic oxindole pyrrolidine, we have conducted DFT calculations. We have employed long-range corrected hybrid density ωB97X-D functional for geometrical optimizations,[28] and 6-31G* basis set. Energies were refined with Minnesota functional MN15,[29] using Karlsruhe triple-zeta def2-TZVP basis set.[30] The solvent effects of DCM were accounted for by the polarizable continuum model (PCM) using the integral equation formalism variant (IEFPCM).[31] This functional accounts for long-range London dispersion effects.

The calculations support the notion that spirocyclization is a two-step process comprising a Michael addition of a carbanion formed from oxindole imine to either keto ester or keto amide.

Table 4. Functional group effect – keto amides.

Entry	R (**5a-d**)	Yield of **6** [%]	ee of **6** [%]	Yield of **7** [%]	ee of **7** [%]
1	NMe_2 (**a**)	36[a]	18	24	19
2	NHMe (**b**)	68	0	5	0
3	$N(CH_2)_4$ (**c**)	20	10	33	26
4	NHBn (**d**)	61	4	0	–

[a] The sum of three diastereoisomers that were isolated with the total dr 4:3:2 and 0–18% ee. Their revised structures are shown in SI.

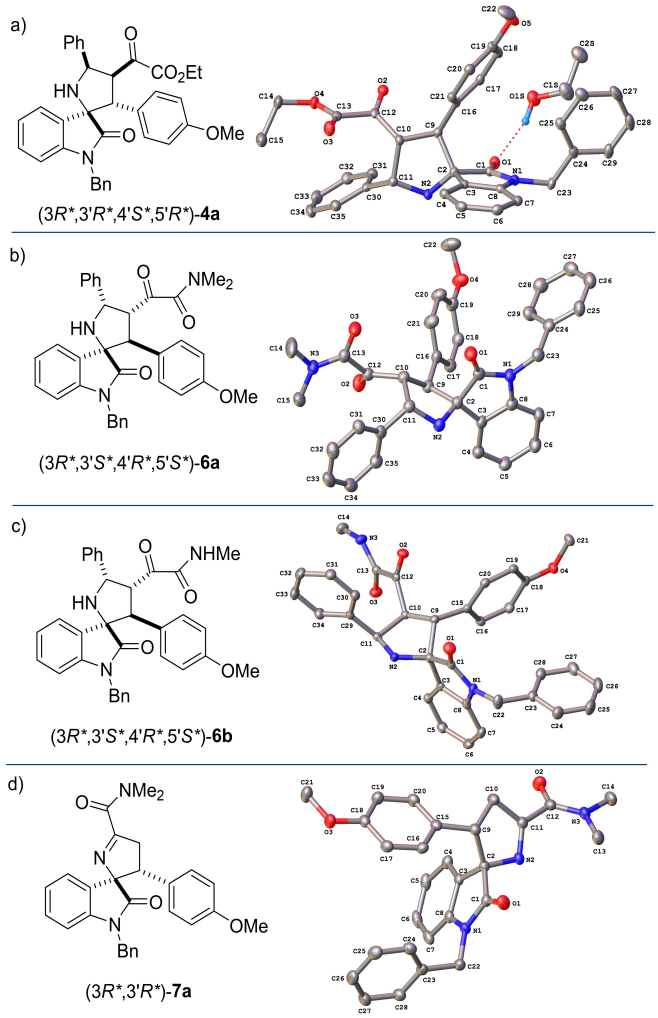

Figure 3. X-Ray crystallographic structures of compounds **4a**, **6a**, **6b**, and **7a**.

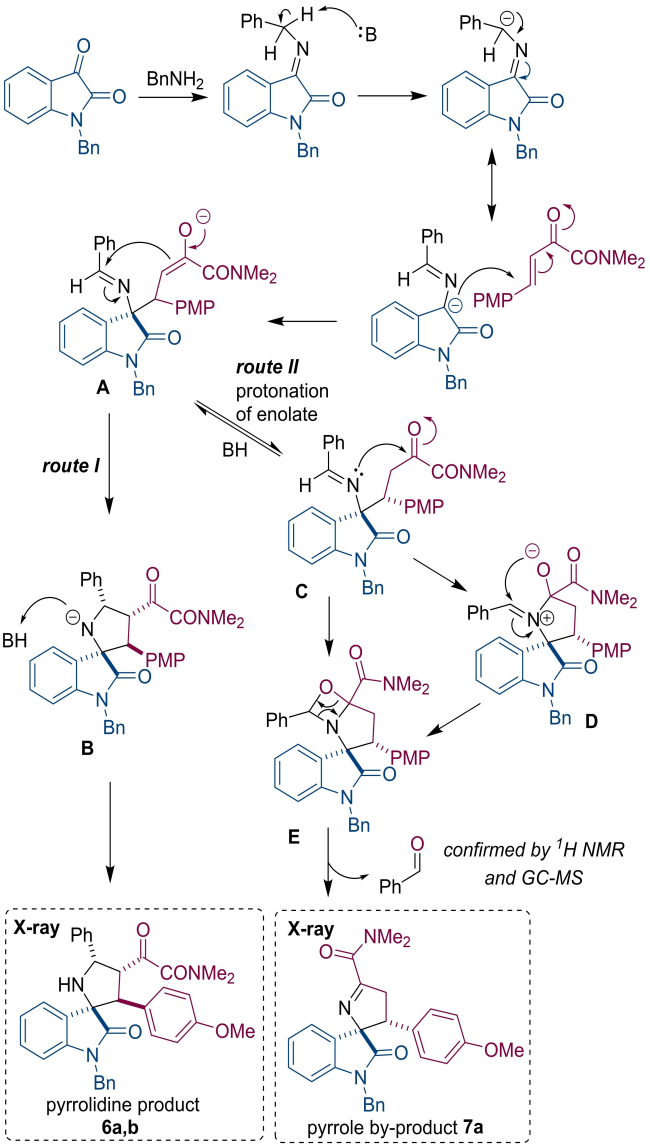

Scheme 3. Proposed reaction mechanism (PMP = *p*-MeO–C_6H_4).

The enolate, which is formed in this step, is then cyclized via addition to imine functionality (Figure 4).

Calculations also support creating the pyrrole by-product **7** via the formation of 1,3-oxazetidine intermediate **E** either via [2 + 2]-type cycloaddition or a stepwise process. Oxazetidine intermediate **E** then decomposes via a retro [2 + 2] cycloaddition to release product **7a** and benzaldehyde. The structure of the product **7a** was unambiguously confirmed by X-ray crystallographic analysis. Figure 5 depicts DFT calculated transition states for the formation of 1,3-oxazetidine intermediate **E** (**TS-[2 + 2]**) and for its decomposition to pyrrole derivative **7a** (**TS-retro-[2 + 2]**).

We have also calculated concerted [3 + 2] cycloaddition reactions from neutral ylide; see SI for more details.

Conclusion

We have shown that *in situ* formed oxindole imines react with unsaturated keto esters and keto amides to provide spirocyclic oxindole pyrrolidines. Chiral quinine-based squaramide organocatalyst can provide ketoester product with an enantiomeric purity of 60% ee, which can be augmented by re-crystallization up to 72% ee. Interestingly, keto amides also afford alternative cyclization product with spirocyclic pyrrole moiety. The identity of keto ester and keto amide spiro-oxindol pyrrolidines, as well as alternative spiro-pyrrole product, were confirmed by X-ray crystallographic analyses, and mechanistic details were elucidated by DFT calculations.

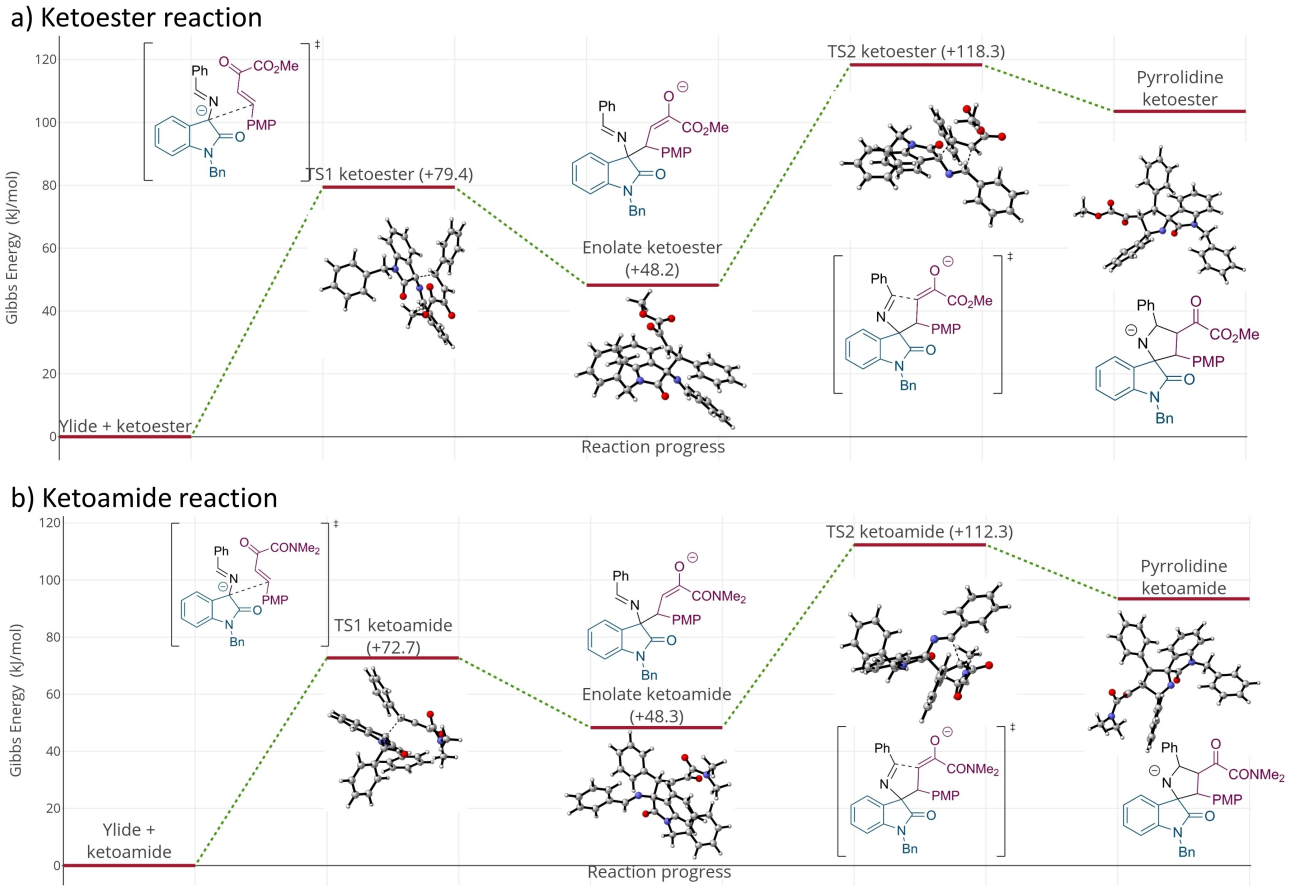

Figure 4. Reaction profiles calculated at ωB97X-D/6-31G*//MN15/def2-TZVP (DCM) level.

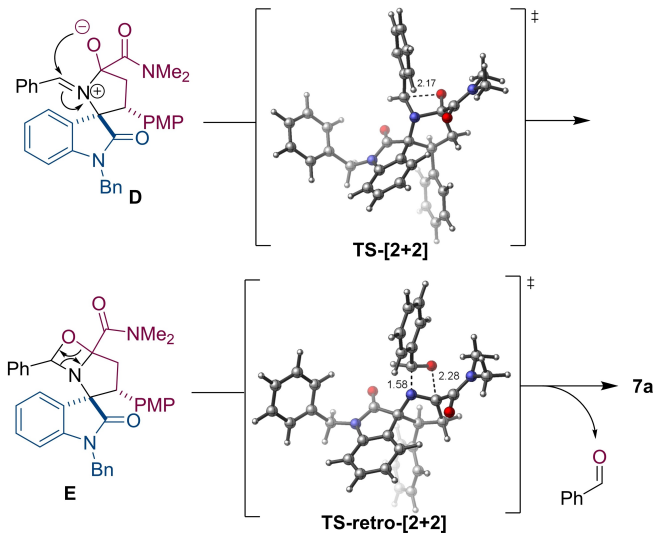

Figure 5. Transition states calculated at ωB97X-D/6-31G*//MN15/def2-TZVP (DCM) level. Molecular models rendered with CYLview20.[32]

Experimental Section

Representative procedure for the synthesis of spiro oxindole pyrrolidines

To a mixture of isatine **1** (1.0 equiv; 0.126 mmol) and MgSO4 (10 equiv; 1.26 mmol) in DCM (1.5 mL) benzylamine (1.1 equiv; 0.139 mmol) was added in one portion under stirring at −5 to 0 °C. After 10 min mixture of ketoester/ketoamide **3** or **5** (1.0 equiv; 0.126 mmol) and catalyst **C** (10 mol%) in DCM (1.5 mL) was added. The reaction mixture was then gradually warm to room temperature and stirred for 24 h. The solvent was evaporated *in vacuo* and the crude reaction mixture was purified by column chromatography on SiO_2 (hexane/EtOAc 3:1→1:1).

Characterization data

Ethyl 2-((3R,3′R,4′S,5′R)-1-benzyl-3′-(4-methoxyphenyl)-2-oxo-5′-phenylspiro[indoline-3,2′-pyrrolidin]-4′-yl)-2-oxoacetate (4a)

White solid; yield of 57% (35 mg), 60% ee (72% ee after recrystallization in abs. EtOH at 5 °C); $[\alpha]_D^{20}$ +83.2 ($CHCl_3$, c 0.25); R_f (hexane/EtOAc, 3:1) 0.27; m.p. 144–146 °C; ^{1}H NMR (600 MHz, $CDCl_3$): δ 7.71 (d, J = 6.7 Hz, 1H), 7.55 (d, J = 7.5 Hz, 2H), 7.35 (t, J = 7.5 Hz, 2H), 7.29–7.27 (m, 1H), 7.21–7.08 (m, 5H), 6.90 (d, J = 8.5 Hz, 2H), 6.83 (d, J = 7.3 Hz, 2H), 6.52 (d, J = 8.5 Hz, 2H), 6.44 (d, J = 7.2 Hz, 1H), 5.53 (d, J = 10.6 Hz, 1H), 5.11–5.06 (m, 2H), 4.55 (d, J = 6.9 Hz, 1H), 4.52 (d, J = 3.4 Hz, 1H), 4.06–4.00 (m, 2H), 3.67 (s, 3H),

2.84 (s, 1H), 1.13 (t, J=7.1 Hz, 3H). ^{13}C NMR (151 MHz, $CDCl_3$): δ 190.9, 177.0, 160.7, 158.8, 142.1, 139.9, 134.9, 131.1, 129.5, 129.0, 128.9, 128.5, 128.4, 128.4, 127.3, 126.8, 126.3, 124.3, 122.6, 113.4, 109.6, 72.6, 63.5, 62.4, 56.8, 55.0, 54.9, 43.9, 13.7. HRMS-ESI$^+$ (*m/z*): calculated for $[C_{35}H_{33}N_2O_5]^+$: 561.2389, found: 561.2384. IR (ATR): 3325 (w), 1701 (s), 1611 (m), 1514 (m), 1456 (m), 1370 (m), 1249 (s), 1176 (s), 1029 (m), 753 (s), 701 (s), 598 (m), 546 (m), 478 (m) cm^{-1}. HPLC: Chiralpak IB, *n*-hexane/*i*-PrOH 90:10, 1 mL/min, 215 nm, t_R= 25.02 and 30.82 min.

Benzyl 2-((3R,3′R,4′S,5′R)-1-benzyl-3′-(4-methoxyphenyl)-2-oxo-5′-phenylspiro[indoline-3,2′-pyrrolidin]-4′-yl)-2-oxoacetate (4b)

Pale yellow solid; yield of 43% (34 mg), 30% ee; $[\alpha]_D^{20}$ + 3.2 ($CHCl_3$, c 0.18); R_f (hexane/EtOAc, 3:1) 0.29; m.p. 73–74 °C; ^{1}H NMR (600 MHz, $CDCl_3$): δ 7.73–7.66 (m, 1H), 7.49 (d, J=7.2 Hz, 2H), 7.37–7.32 (m, 3H), 7.28–7.07 (m, 10H), 6.90 (d, J=8.7 Hz, 2H), 6.83 (d, J=7.2 Hz, 2H), 6.52 (d, J=8.7 Hz, 2H), 6.47–6.42 (m, 1H), 5.52 (d, J=10.5 Hz, 1H), 5.15–5.05 (m, 2H), 5.00 (q, J=12.1 Hz, 2H), 4.53 (d, J=13.7 Hz, 2H), 3.66 (s, 3H), 2.86 (s, 1H). ^{13}C NMR (151 MHz, $CDCl_3$): δ 187.8, 174.5, 157.9, 156.2, 139.5, 137.2, 132.4, 131.6, 128.5, 126.9, 126.4, 126.3, 126.1, 126.1, 126.0, 125.9, 125.9, 125.7, 124.8, 124.3, 123.6, 121.7, 120.1, 110.8, 107.1, 70.0, 65.4, 60.9, 54.4, 52.5, 52.3, 41.3. HRMS-ESI$^+$ (*m/z*): calculated for $[C_{40}H_{34}N_2O_5K]^+$: 661.2100, found: 661.2101. IR (ATR): 2930 (w), 1717 (s), 1610 (m), 1513 (m), 1455 (m), 1247 (m), 1176 (m), 1028 (m), 750 (s), 696 (s), 543 (w) cm^{-1}. HPLC: Chiralpak IB, *n*-hexane/*i*-PrOH 90:10, 1 mL/min, 215 nm, t_R=19.87 and 23.35 min.

Methyl 2-((3R,3′R,4′S,5′R)-1-benzyl-3′-(4-methoxyphenyl)-2-oxo-5′-phenylspiro[indoline-3,2′-pyrrolidin]-4′-yl)-2-oxoacetate (4c)

Pale yellow solid; yield of 71% (49 mg), 28% ee; $[\alpha]_D^{20}$ + 17.2 ($CHCl_3$, c 0.35); R_f (hexane/EtOAc, 3:1) 0.29; m.p. 130–132 °C; ^{1}H NMR (600 MHz, $CDCl_3$): δ 7.73–7.68 (m, 1H), 7.55 (d, J=7.4 Hz, 2H), 7.35 (t, J=7.6 Hz, 2H), 7.28 (d, J=7.4 Hz, 1H), 7.21–7.05 (m, 5H), 6.90 (d, J=8.7 Hz, 2H), 6.83 (d, J=7.1 Hz, 2H), 6.52 (d, J=8.7 Hz, 2H), 6.46–6.42 (m, 1H), 5.53 (d, J=10.6 Hz, 1H), 5.13–5.04 (m, 2H), 4.55 (d, J=3.1 Hz, 1H), 4.52 (s, 1H), 3.66 (s, 3H), 3.57 (s, 3H), 2.91 (s, 1H). ^{13}C NMR (151 MHz, $CDCl_3$): δ 190.5, 177.0, 161.1, 158.8, 142.1, 139.8, 135.0, 131.0, 129.5, 129.0, 128.9, 128.6, 128.5, 128.3, 127.4, 126.8, 126.2, 124.3, 122.7, 113.4, 109.7, 72.6, 63.5, 57.0, 55.0, 54.8, 52.9, 43.9. HRMS-ESI$^+$ (*m/z*): calculated for $[C_{34}H_{31}N_2O_5]^+$: 547.2227, found: 547.2230. IR (ATR): 3326 (w), 2922 (w), 2852 (w), 1709 (s), 1610 (m), 1513 (m), 1465 (m), 1367 (m), 1249 (s), 1174 (s), 1029 (m), 752 (s), 701 (s), 597 (m), 546 (m), 477 (m) cm^{-1}. HPLC: Chiralpak IC, *n*-hexane/*i*-PrOH 90:10, 1 mL/min, 215 nm, t_R=72.36 and 81.03 min.

Tert-butyl 2-((3R,3′R,4′S,5′R)-1-benzyl-3′-(4-methoxyphenyl)-2-oxo-5′-phenylspiro[indoline-3,2′-pyrrolidin]-4′-yl)-2-oxoacetate (4d)

Pale yellow solid; yield of 87% (65 mg), 52% ee; $[\alpha]_D^{20}$ + 11.2 ($CHCl_3$, c 0.50); R_f (hexane/EtOAc, 3:1) 0.39; m.p. 93–94 °C; ^{1}H NMR (600 MHz, $CDCl_3$): δ 7.73–7.68 (m, 1H), 7.55 (d, J=7.4 Hz, 2H), 7.34 (t, J=7.6 Hz, 2H), 7.28–7.25 (m, 1H), 7.20–7.05 (m, 5H), 6.90 (d, J=8.7 Hz, 2H), 6.80 (d, J=7.3 Hz, 2H), 6.52 (d, J=8.7 Hz, 2H), 6.44–6.40 (m, 1H), 5.52 (d, J=10.5 Hz, 1H), 5.13–5.03 (m, 2H), 4.53–4.49 (m, 2H), 3.66 (s, 3H), 2.84 (s, 1H), 1.32 (s, 9H). ^{13}C NMR (151 MHz, $CDCl_3$): δ 191.7, 177.1, 159.8, 158.8, 142.1, 140.2, 135.0, 131.2, 129.6, 129.0, 128.9, 128.5, 128.5, 128.3, 127.3, 126.8, 126.4, 124.4, 122.6, 113.4, 109.6, 83.7, 72.6, 63.6, 56.6, 55.3, 55.0, 43.9, 27.5. HRMS-ESI$^+$ (*m/z*): calculated for $[C_{37}H_{36}N_2O_5K]^+$: 627.2256, found: 627.2260. IR (ATR): 3346 (w), 2973 (w), 2932 (w), 1711 (s), 1610 (m), 1513 (m), 1367 (m), 1247 (s), 1174 (m), 1029 (s), 830 (m), 751 (s), 698 (s), 543 (m) cm^{-1}. HPLC: Chiralpak IC, *n*-hexane/*i*PrOH 90:10, 1 mL/min, 215 nm, t_R= 32.33 and 39.96 min.

Ethyl 2-((3R,3′R,4′S,5′R)-1-benzyl-3′-(4-bromophenyl)-2-oxo-5′-phenylspiro[indoline-3,2′-pyrrolidin]-4′-yl)-2-oxoacetate (4e)

White solid; yield of 35% (27 mg); $[\alpha]_D^{20}$ −57.5 ($CHCl_3$, c 0.50); R_f (hexane/EtOAc, 3:1) 0.33; m.p. 159–160 °C; ^{1}H NMR (600 MHz, $CDCl_3$): δ 7.70 (dd, J=5.5, 3.1 Hz, 1H), 7.53 (d, J=7.5 Hz, 2H), 7.36 (t, J=7.6 Hz, 2H), 7.28 (t, J=7.3 Hz, 1H), 7.24–7.18 (m, 3H), 7.13 (dd, J=5.5, 3.1 Hz, 2H), 7.11 (d, J=8.4 Hz, 2H), 6.85 (d, J=8.4 Hz, 2H), 6.81 (d, J=6.4 Hz, 2H), 6.50–6.46 (m, 1H), 5.54 (d, J=10.6 Hz, 1H), 5.14–5.01 (m, 2H), 4.58–4.46 (m, 2H), 4.09–3.97 (m, 2H), 2.84 (s, 1H), 1.13 (t, J=7.1 Hz, 3H). ^{13}C NMR (151 MHz, $CDCl_3$): δ 190.7, 176.6, 160.7, 142.0, 139.6, 134.8, 133.4, 131.1, 130.5, 130.1, 129.3, 128.9, 128.6, 128.6, 128.3, 127.5, 126.7, 124.3, 122.8, 121.5, 109.8, 72.4, 63.5, 62.5, 56.8, 55.0, 43.9, 13.7. HRMS-ESI$^+$ (*m/z*): calculated for $[C_{34}H_{29}BrN_2O_4K]^+$: 647.0942 and 649.0922, found: 647.0942 and 649.0920 (both isotopes of Bromine) IR (ATR): 2962 (w), 2925 (w), 1717 (s), 1610 (m), 1488 (m), 1466 (m), 1364 (m), 1246 (m), 1174 (m), 1074 (m), 1029 (s), 1009 (s), 800 (m), 751 (s), 729 (s), 696 (s), 489 (w) cm^{-1}. HPLC: *conditions not found.*

Benzyl 2-((3R,3′R,4′S,5′R)-1-benzyl-3′-(4-bromophenyl)-2-oxo-5′-phenylspiro[indoline-3,2′-pyrrolidin]-4′-yl)-2-oxoacetate (4f)

White solid; yield of 27% (23 mg); $[\alpha]_D^{20}$ −88.4 ($CHCl_3$, c 0.20); R_f (hexane/EtOAc, 3:1) 0.41; m.p. 133–134 °C; ^{1}H NMR (600 MHz, $CDCl_3$): δ 7.69–7.67 (m, 1H), 7.47 (d, J=7.1 Hz, 2H), 7.37–7.32 (m, 3H), 7.28–7.18 (m, 9H), 7.14–7.12 (m, 2H), 7.10 (d, J=8.4 Hz, 2H), 6.83 (d, J=8.4 Hz, 2H), 6.81 (d, J=6.5 Hz, 2H), 6.48–6.47 (m, 1H), 5.52 (d, J=10.5 Hz, 1H), 5.12–5.04 (m, 2H), 5.00 (q, J=12.1 Hz, 2H), 4.54–4.48 (m, 2H). ^{13}C NMR (151 MHz, $CDCl_3$): δ 190.2, 176.6, 160.4, 142.0, 139.6, 134.8, 134.1, 133.3, 131.1, 130.6, 130.1, 129.3, 128.9, 128.7, 128.7, 128.6, 128.6, 128.2, 127.5, 126.7, 124.3, 122.8, 121.5, 109.8, 72.4, 68.0, 63.4, 56.8, 55.0, 43.9. HRMS-ESI$^+$ (*m/z*): calculated for $[C_{39}H_{32}N_2O_4]^+$: 671.1540 and 673.1519, found: 671.1544 and 673.1520. (both isotopes of Bromine) IR (ATR): 3033 (w), 2957 (w). 2925 (w), 1717 (s), 1611 (m), 1489 (m), 1467 (m), 1363 (m), 1279 (m), 1279 (m), 1243 (m), 1175 (m), 1074 (m), 1010 (m), 750 (m), 731 (m), 695 (s) cm^{-1}. HPLC: *conditions not found.*

2-((3R,3′S,4′R,5′R)-1-Benzyl-3′-(4-methoxyphenyl)-2-oxo-5′-phenylspiro[indoline-3,2′-pyrrolidin]-4′-yl)-N,N-dimethyl-2-oxoacetamide ((R,S,R,R)-6a)

White solid; yield of 8% (6 mg), 4% ee; R_f (hexane/EtOAc 1:1) 0.62; m.p. 184–186 °C; ^{1}H NMR ($CDCl_3$, 600 MHz): δ 7.46 (m, 2H), 7.41 (d, J=7.3 Hz, 1H), 7.33 (m, 2H), 7.29 (m, 2H), 7.28–7.20 (m, 6H), 7.15 (t, J=7.7 Hz, 1H), 7.04 (t, J=7.5 Hz, 1H), 6.78 (d, J=8.7 Hz, 2H), 6.65 (d, J=7.7 Hz, 1H), 4.99 (d, J=15.8 Hz, 1H), 4.98 (d, J=10.4 Hz, 1H), 4.93 (d, J=15.8 Hz, 1H), 4.81 (d, J=11.5 Hz, 1H), 3.81 (t, J=11.1 Hz, 1H), 3.75 (s, 3H), 2.59 (br.s, 1H), 2.49 (s, 3H), 2.46 (s, 3H). ^{13}C NMR ($CDCl_3$, 151 MHz): δ 196.4, 180.6, 163.4, 158.7, 143.6, 140.7, 135.8, 130.4, 130.3, 129.6, 129.5, 128.8, 128.4, 127.8, 127.2, 125.3, 122.9, 114.0, 109.4, 68.4, 67.2, 63.1, 55.3, 54.7, 44.7, 36.6, 35.6. HRMS-ESI$^+$ (*m/z*): calculated for $[C_{35}H_{34}N_3O_4]^+$: 560.2544; found: 560.2545. IR (ATR): 3331 (w), 3030 (w), 2929 (w), 1710 (s), 1641 (s), 1610 (s), 1513 (s), 1487 (s), 1466 (s), 1352 (s), 1303 (m), 1248 (s), 1176 (s), 1114 (m), 1080 (m), 1029 (s), 833 (m), 808 (m), 732 (s), 698 (s), 550 (m) cm^{-1}. HPLC: Chiralpak IB, *n*-hexane/*i*-PrOH 95:5, 1.2 mL/min, 215 nm, t= 24.97 and 42.49 min.

2-((2′R,3′S,4′R,5′S)-1-Benzyl-3′-(4-methoxyphenyl)-2-oxo-5′-phenylspiro[indoline-3,2′-pyrrolidine]-4′-yl)-N,N-dimethyl-2-oxo-acetamide ((R,S,R,S)-6 a)

White solid; yield of 12% (8 mg), 18% ee; R_f (hexane/EtOAc 1:1) 0.55; m.p. 195–197 °C; ^{1}H NMR ($CDCl_3$, 600 MHz): δ 7.75 (d, J= 7.0 Hz, 1H), 7.63 (d, J=7.2 Hz, 2H), 7.36 (t, J=7.6 Hz, 2H), 7.26 (m, 1H), 7.18–7.12 (m, 3H), 7.08 (t, J=7.5 Hz, 2H), 6.99 (d, J=8.7 Hz, 2H), 6.64 (d, J=8.8 Hz, 2H), 6.45 (d, J=7.5 Hz, 2H), 6.37 (d, J=8.1 Hz, 1H), 5.85 (t, J=11.3 Hz, 1H), 5.77 (d, J=11.0 Hz, 1H), 5.10 (d, J= 16.1 Hz, 1H), 4.32 (d, J=11.7 Hz, 1H), 4.20 (d, J=16.1 Hz, 1H), 3.72 (s, 3H), 2.71 (s, 3H), 2.61 (br.s, 1H), 2.16 (s, 3H). ^{13}C NMR ($CDCl_3$, 151 MHz): δ 198.0, 179.1, 164.5, 159.2, 143.4, 142.1, 135.2, 129.7, 129.4, 129.3, 128.8, 128.5, 128.1, 127.3, 126.9, 126.6, 123.8, 123.0, 113.9, 109.4, 72.5, 60.4, 55.2, 53.6, 53.2, 43.5, 36.5, 35.8. HRMS-ESI$^+$ (*m/z*): calculated for $[C_{35}H_{34}N_3O_4]^+$: 560.2544; found: 560.2548. IR (ATR): 3338 (w), 2925 (w), 1708 (s), 1634 (s), 1612 (s), 1513 (m), 1489 (m), 1467 (m), 1355 (s), 1312 (m), 1247 (s), 1178 (s), 1131 (m), 1057 (m), 1029 (s), 995 (s), 845 (m), 826 (m), 796 (m), 779 (m), 745 (s), 734 (s), 698 (s), 676 (s), 641 (m), 624 (s), 577 (s), 543 (s), 515 (m) cm^{-1}. HPLC: Chiralcel OD-H, *n*-hexane/*i*PrOH 90:10, 1.0 mL/min, 215 nm, t_R=40.92 and 48.07 min.

2-((2′R,3′R,4′S,5′R)-1-Benzyl-3′-(4-methoxyphenyl)-2-oxo-5′-phenylspiro[indoline-3,2′-pyrrolidine]-4′-yl)-N,N-dimethyl-2-oxo-acetamide ((R,R,S,R)-6 a)

White solid; yield of 16% (11 mg), 16% ee; $[\alpha]_D^{20}$ −122.3 ($CHCl_3$, c 0.15); R_f (hexane/EtOAc 1:1) 0.38; m.p. 173–175 °C; ^{1}H NMR ($CDCl_3$, 600 MHz): δ 7.68 (m, 3H), 7.37 (t, J=7.7 Hz, 2H), 7.28 (t, J=7.4 Hz, 1H), 7.19-7.15 (m, 3H), 7.08 (m, 2H), 6.93 (d, J=8.7 Hz, 2H), 6.87 (d, J=6.7 Hz, 2H), 6.52 (d, J=8.8 Hz, 2H), 6.42 (m, 1H), 5.46–5.39 (m, 2H), 5.08 (d, J=16.0 Hz, 1H), 4.57 (d, J=16.0 Hz, 1H), 4.48 (d, J= 12.7 Hz, 1H), 3.66 (s, 3H), 2.76 (s, 3H), 2.19 (s, 3H). ^{13}C NMR ($CDCl_3$, 151 MHz): δ 196.1, 177.7, 164.3, 158.8, 142.1, 141.5, 135.2, 131.5, 129.4, 129.0, 128.8, 128.7, 128.6, 128.4, 127.5, 127.0, 126.9, 124.5, 122.8, 113.5, 109.6, 72.6, 62.5, 55.8, 55.2, 54.7, 44.1, 36.6, 36.0. HRMS-ESI$^+$ (*m/z*): calculated for $[C_{35}H_{34}N_3O_4]^+$: 560.2544; found: 560.2548. IR (ATR): 3355 (w), 3189 (w), 2919 (s), 2850 (m), 1711 (s), 1637 (s), 1609 (s), 1512 (s), 1487 (m), 1466 (s), 1408 (m), 1362 (m), 1247 (s), 1174 (s), 1101 (m), 1077 (m), 1029 (s), 829 (m), 807 (m), 752 (s), 697 (s), 543 (s) cm^{-1}. HPLC: Chiralpak IB, *n*-hexane/*i*PrOH 90:10, 1.0 mL/min, 215 nm, t_R=24.30 and 31.92 min.

(2′R,3′R)-1-benzyl-3′-(4-methoxyphenyl)-N,N-dimethyl-2-oxo-3′,4′-dihydrospiro[indoline-3,2′-pyrrole]-5′-carboxamide (7 a)

White solid; yield of 24% (14 mg), 19% ee; $[\alpha]_D^{20}$ −82.9 ($CHCl_3$, c 0.28); R_f (hexane/EtOAc 1:1) 0.18; R_f (EtOAc) 0.59; m.p. 195–196 °C; ^{1}H NMR ($CDCl_3$, 600 MHz): δ 7.32–7.27 (m, 3H), 7.23 (d, J=7.0 Hz, 2H), 7.04 (t, J=7.8 Hz, 1H), 6.96 (d, J=8.6 Hz, 2H), 6.74 (t, J=7.6 Hz, 1H), 6.67 (d, J=8.7 Hz, 2H), 6.60 (d, J=7.8 Hz, 1H), 6.51 (d, J= 7.5 Hz, 1H), 5.08 (d, J=15.8 Hz, 1H), 4.77 (d, J=15.8 Hz, 1H), 4.07 (dd, J=8.2, 6.9 Hz, 1H), 3.72 (s, 3H), 3.69 (dd, J=17.8, 6.7 Hz, 1H), 3.61 (dd, J=17.7, 8.4 Hz, 1H), 3.26 (s, 3H), 3.09 (s, 3H). ^{13}C NMR ($CDCl_3$, 151 MHz): δ 176.5, 175.9, 165.3, 158.8, 142.7, 135.5, 130.1, 129.3, 129.3, 128.9, 127.8, 127.3, 126.9, 126.0, 122.7, 113.8, 109.3, 86.2, 55.3, 50.5, 44.1, 43.9, 38.4, 35.1. HRMS-ESI$^+$ (*m/z*): calculated for $[C_{28}H_{27}N_3O_3Na]^+$: 476.1945; found: 476.1942. IR (ATR): 3039 (w), 2931 (w), 2831 (w), 1710 (s), 1634 (s), 1609 (s), 1513 (s), 1487 (s), 1468 (s), 1442 (m), 1410 (m), 1362 (s), 1344 (s), 1305 (m), 1240 (s), 1205 (m), 1174 (s), 1148 (m), 1114 (m), 1075 (s), 1035 (m), 949 (m), 915 (m), 876 (m), 829 (s), 803 (m), 757 (s), 720 (m), 698 (s), 628 (s), 591 (s), 546 (s) cm^{-1}. HPLC: Chiralpak IC, *n*-hexane/*i*-PrOH 90:10, 1.0 mL/min, 211 nm, t_R=78.33 and 89.16 min.

2-((2′R,3′R,4′S,5′R)-1-Benzyl-3′-(4-methoxyphenyl)-2-oxo-5′-phenylspiro[indoline-3,2′-pyrrolidine]-4′-yl)-N-methyl-2-oxo-acetamide (6 b)

White solid; yield of 68% (47 mg), 0% ee; R_f (hexane/EtOAc 1:1) 0.51; m.p. 155–156 °C; ^{1}H NMR ($CDCl_3$, 600 MHz): δ 7.75 (d, J= 6.9 Hz, 1H), 7.62 (d, J=7.3 Hz, 2H), 7.32 (t, J=7.6 Hz, 2H), 7.23 (t, J= 7.3 Hz, 1H), 7.20–7.14 (m, 3H), 7.13-7.07 (m, 2H), 6.88 (d, J=8.7 Hz, 2H), 6.84 (d, J=7.2 Hz, 2H), 6.51 (d, J=8.7 Hz, 2H), 6.43 (d, J= 8.3 Hz, 1H), 6.26 (d, J=5.1 Hz, 1H), 5.61 (d, J=10.4 Hz, 1H), 5.31 (dd, J=13.1, 10.4 Hz, 1H), 5.09 (d, J=16.0 Hz, 1H), 4.54 (d, J=16.0 Hz, 1H), 4.49 (d, J=13.2 Hz, 1H), 3.66 (s, 3H), 2.85 (s, 1H), 2.64 (d, J= 5.2 Hz, 3H). ^{13}C NMR ($CDCl_3$, 151 MHz): δ 195.9, 177.7, 160.9, 158.9, 142.1, 140.9, 135.2, 131.4, 129.6, 129.1, 128.7, 128.6, 128.5, 128.2, 127.5, 127.0, 126.5, 124.6, 122.8, 113.5, 109.7, 72.8, 63.5, 55.2, 54.7, 54.6, 44.1, 25.8. HRMS-ESI$^+$ (*m/z*): calculated for $[C_{34}H_{32}N_3O_4]^+$: 546.2387; found: 546.2392. IR (ATR): 3383 (w), 3065 (w), 3034 (w), 3001 (w), 2936 (w), 1736 (m), 1711 (s), 1683 (s), 1612 (m), 1583 (m), 1515 (s), 1496 (m), 1466 (m), 1437 (m), 1373 (m), 1248 (s), 1181 (s), 1112 (m), 1029 (m), 1011 (m), 989 (m), 935 (m), 901 (m), 830 (s), 775 (s), 754 (s), 727 (m), 701 (s), 600 (m), 546 (m) cm^{-1}. HPLC: Chiralpak IC, *n*-hexane/*i*PrOH 90:10, 1.0 mL/min, 215 nm, t_R=57.76 and 92.63 min.

(2′R,3′R)-1-benzyl-3′-(4-methoxyphenyl)-N-methyl-2-oxo-3′,4′-dihydrospiro[indoline-3,2′-pyrrole]-5′-carboxamide (7 b)

White solid; yield of 5% (3 mg), 0% ee; R_f (hexane/EtOAc 1:1) 0.38; m.p. 135–136 °C; ^{1}H NMR ($CDCl_3$, 600 MHz): δ 7.31–7.26 (m, 3H), 7.20 (d, J=7.0 Hz, 2H), 7.14 (d, J=4.3 Hz, 1H), 7.06 (t, J=7.7 Hz, 1H), 6.89 (d, J=8.5 Hz, 2H), 6.81 (t, J=7.5 Hz, 1H), 6.70 (d, J=7.4 Hz, 1H), 6.61 (d, J=8.6 Hz, 2H), 6.59 (d, J=7.9 Hz, 1H), 5.09 (d, J=15.7 Hz, 1H), 4.77 (d, J=15.7 Hz, 1H), 4.23 (t, J=9.0 Hz, 1H), 3.70 (s, 3H), 3.65 (dd, J=18.3, 8.6 Hz, 1H), 3.56 (dd, J=18.2, 9.4 Hz, 1H), 2.93 (d, J=5.1 Hz, 3H). ^{13}C NMR ($CDCl_3$, 151 MHz): δ 176.4, 175.6, 162.3, 158.8, 142.5, 135.4, 129.7, 129.0, 128.9, 128.7, 127.8, 127.4, 126.6, 125.5, 122.7, 113.7, 109.6, 85.4, 55.3, 51.3, 44.2, 40.3, 26.1. HRMS-ESI$^+$ (*m/z*): calculated for $[C_{27}H_{25}N_3O_3Na]^+$: 462.1788; found: 462.1788. IR (ATR): 3386 (w), 2967 (w), 2932 (w), 1714 (s), 1678 (s), 1608 (s), 1542 (m), 1515 (m), 1489 (s), 1467 (s), 1431 (m), 1354 (s), 1309 (m), 1256 (s), 1176 (s), 1145 (m), 1118 (m), 1022 (s), 959 (s), 904 (w), 834 (s), 796 (m), 762 (s), 727 (s), 706 (s), 598 (s) cm^{-1}. HPLC: Chiralpak IB, *n*-hexane/*i*-PrOH 95:5, 1.2 mL/min, 215 nm, t=57.24 and 71.02 min.

1-((2′R,3′R,4′S,5′R)-1-Benzyl-3′-(4-methoxyphenyl)-2-oxo-5′-phenylspiro[indoline-3,2′-pyrrolidine]-4′-yl)-2-(pyrrolidin-1-yl) ethane-1,2-dione (6 c)

White solid; yield of 20% (15 mg), 10% ee; $[\alpha]_D^{20}$ −77.1 ($CHCl_3$, c 0.28); R_f (hexane/EtOAc 1:1) 0.34; m.p. 120–121 °C; ^{1}H NMR ($CDCl_3$, 600 MHz): δ 7.72 (d, J=6.8 Hz, 1H), 7.64 (d, J=7.2 Hz, 2H), 7.34 (t, J=7.6 Hz, 2H), 7.26 (m, 1H), 7.18 (m, 3H), 7.11–7.06 (m, 2H), 6.93 (d, J=8.7 Hz, 2H), 6.86 (d, J=6.9 Hz, 2H), 6.53 (d, J=8.8 Hz, 2H), 6.42 (d, J=8.5 Hz, 1H), 5.50 (d, J=10.7 Hz, 1H), 5.44 (dd, J=12.7, 10.7 Hz, 1H), 5.08 (d, J=16.0 Hz, 1H), 4.56 (d, J=16.0 Hz, 1H), 4.47 (d, J= 12.8 Hz, 1H), 3.66 (s, 3H), 3.32 (m, 1H), 3.25–3.19 (m, 2H), 2.23 (m, 1H), 1.69-1.56 (m, 4H), 1.41 (m, 1H). ^{13}C NMR ($CDCl_3$, 151 MHz): δ 196.7, 177.6, 161.3, 158.8, 142.1, 141.6, 135.2, 131.5, 129.5, 129.0, 128.7, 128.7, 128.1, 127.5, 127.0, 127.0, 124.6, 122.8, 113.5, 109.6, 72.7, 62.7, 55.8, 55.2, 54.5, 46.9, 46.8, 44.1, 26.4, 23.4. HRMS-ESI$^+$ (*m/z*): calculated for $[C_{37}H_{36}N_3O_4]^+$: 586.2700; found: 586.2703. IR (ATR): 3332 (w), 2962 (w), 1716 (s), 1631 (s), 1610 (s), 1513 (s), 1487 (m), 1454 (s), 1362 (s), 1249 (s), 1176 (s), 1100 (s), 1078 (s), 1028 (s), 910 (m), 862 (m), 798 (s), 752 (s), 729 (s), 698 (s), 592 (m) cm^{-1}. HPLC:

Chiralpak IB, *n*-hexane/*i*-PrOH 90:10, 1.0 mL/min, 215 nm, t_R = 26.85 and 36.26 min.

(2′R,3′R)-1-Benzyl-3′-(4-methoxyphenyl)-5′-(pyrrolidine-1-carbonyl)-3′,4′-dihydrospiro[indoline-3,2′-pyrrol]-2-one (7c)

White solid; yield of 33% (21 mg), 26% ee; $[\alpha]_D^{20}$ −92.7 ($CHCl_3$, c 0.22). R_f (hexane/EtOAc 1:1) 0.20; m.p. 163–165 °C; ^{1}H NMR ($CDCl_3$, 600 MHz): δ 7.30–7.25 (m, 3H), 7.20 (d, *J* = 6.8 Hz, 2H), 7.04 (td, *J* = 7.8, 1.1 Hz, 1H), 6.93 (d, *J* = 8.6 Hz, 2H), 6.78 (t, *J* = 7.6 Hz, 1H), 6.65 (d, *J* = 7.7 Hz, 1H), 6.63 (d, *J* = 8.7 Hz, 2H), 6.58 (d, *J* = 7.8 Hz, 1H), 5.11 (d, *J* = 15.8 Hz, 1H), 4.75 (d, *J* = 15.8 Hz, 1H), 4.14–4.10 (m, 1H), 3.80 (m, 2H), 3.71 (s, 3H), 3.70 (dd, *J* = 17.9, 8.5 Hz, 1H), 3.62 (m, 2H), 3.59 (dd, *J* = 17.9, 8.5 Hz, 1H), 1.96-1.85 (m, 4H). ^{13}C NMR ($CDCl_3$, 151 MHz): δ 176.7, 176.3, 162.6, 158.7, 142.6, 135.5, 129.4, 129.4, 129.2, 128.9, 127.74, 127.3, 127.0, 125.7, 122.6, 113.7, 109.3, 86.1, 55.3, 50.4, 48.8, 46.6, 44.1, 43.0, 26.4, 24.1. HRMS-ESI$^+$ (*m/z*): calculated for $[C_{30}H_{29}N_3O_3Na]^+$: 502.2101; found: 502.2102. IR (ATR): 2973 (w), 2948 (w), 2872 (w), 1717 (s), 1599 (s), 1513 (s), 1487 (s), 1450 (s), 1363 (s), 1345 (s), 1305 (m), 1268 (m), 1245 (s), 1175 (s), 1139 (m), 1110 (m), 1079 (m), 1027 (s), 998 (m), 962 (m), 930 (m), 839 (m), 819 (m), 753 (s), 734 (m), 698 (s), 598 (m), 544 (m) cm^{-1}. HPLC: Chiralpak IB, *n*-hexane/*i*-PrOH 95:5, 1.2 mL/min, 215 nm, t_R = 55.23 and 63.17 min.

N-Benzyl-2-((2′R,3′R,4′S,5′R)-1-benzyl-3′-(4-methoxyphenyl)-2-oxo-5′-phenylspiro[indoline-3,2′-pyrrolidine]-4′-yl)-2-oxo-acetamide (6d)

White solid; yield of 61% (48 mg), 4% ee; R_f (hexane/EtOAc 3:1) 0.18; m.p. 134–135 °C; ^{1}H NMR ($CDCl_3$, 600 MHz): δ 7.76 (d, *J* = 6.8 Hz, 1H), 7.61 (d, *J* = 7.4 Hz, 2H), 7.29–7.22 (m, 6H), 7.20–7.14 (m, 3H), 7.13–7.08 (m, 2H), 7.03 (d, *J* = 6.7 Hz, 2H), 6.89 (d, *J* = 8.6 Hz, 2H), 6.84 (d, *J* = 7.3 Hz, 2H), 6.62 (t, *J* = 5.7 Hz, 1H), 6.51 (d, *J* = 8.6 Hz, 2H), 6.43 (d, *J* = 7.3 Hz, 1H), 5.63 (d, *J* = 10.4 Hz, 1H), 5.34 (dd, *J* = 13.0, 10.6 Hz, 1H), 5.09 (d, *J* = 16.0 Hz, 1H), 4.54 (d, *J* = 16.0 Hz, 1H), 4.50 (d, *J* = 13.1 Hz, 1H), 4.33 (dd, *J* = 14.8, 6.7 Hz, 1H), 4.17 (dd, *J* = 14.8, 5.6 Hz, 1H), 3.66 (s, 3H), 2.84 (br s, 1H). ^{13}C NMR ($CDCl_3$, 151 MHz): δ 195.9, 177.6, 160.0, 158.9, 142.1, 140.8, 136.7, 135.2, 131.4, 129.6, 129.1, 128.8, 128.7, 128.7, 128.5, 128.2, 127.9, 127.8, 127.5, 127.0, 126.5, 124.6, 122.8, 113.5, 109.7, 72.8, 63.7, 55.2, 54.8, 54.8, 44.1, 43.3. HRMS-ESI$^+$ (*m/z*): calculated for $[C_{40}H_{36}N_3O_4]^+$: 622.2700; found: 622.2705. IR (ATR): 3330 (w), 3028 (w), 2928 (w), 1717 (s), 1676 (s), 1609 (s), 1512 (s), 1487 (m), 1453 (m), 1358 (m), 1247 (s), 1175 (s), 1127 (m), 1106 (m), 1078 (m), 1028 (m), 981 (m), 830 (m), 750 (s), 696 (s), 593 (m), 543 (m) cm^{-1}. HPLC: Chiralpak IC, *n*-hexane/*i*-PrOH 90:10, 1.0 mL/min, 211 nm, t_R = 54.85 and 78.80 min.

X-ray crystallographic analysis

Crystals for X-ray single-crystal analysis were obtained by slow evaporation from concentrated EtOH, EtOH/1,4-dioxane, or EtOH/EtOAc solutions. The crystallographic experimental data and refinement details are reported in supporting information, Table S2.

Deposition Numbers 2052333 (for **4a**), 2054164 (for **6a**), 2054322 (for **6b**), and 2054327 (for **7a**) contain the supplementary crystallographic data for this paper. These data are provided free of charge by the joint Cambridge Crystallographic Data Centre and Fachinformationszentrum Karlsruhe Access Structures service www.ccdc.cam.ac.uk/structures.

Acknowledgements

This work was supported by the Slovak Research and Development Agency (grant APVV-18-0242). Vitalii Palchykov thanks SAIA and the National Scholarship Programme of the Slovak Republic for an individual scholarship. We thank Dr. Ján Moncoľ from the Slovak University of Technology, Faculty of Chemical and Food Technology for the access to the Cu microsource-equipped diffractometer. This work was supported in part through the Comenius University in Bratislava CLARA@UNIBA.SK high performance computing facilities, services and staff expertise of Centre for Information Technology; https://uniba.sk/en/HPC-Clara.

Conflict of Interest

The authors declare no conflict of interest.

Keywords: Asymmetric organocatalysis · [3 + 2] Cycloaddition · Heterocycles · Pyrrolidine · Spiro oxindole

[1] K. R. Campos, P. J. Coleman, J. C. Alvarez, S. D. Dreher, R. M. Garbaccio, N. K. Terrett, R. D. Tillyer, M. D. Truppo, E. R. Parmee, *Science* **2019**, *363*, eaat0805.
[2] a) A. K. Franz, N. V. Hanhan, N. R. Ball-Jones, *ACS Catal.* **2013**, *3*, 540–553; b) J. Adrio, J. C. Carretero, *Chem. Commun.* **2014**, *50*, 12434–12446; c) F. Meyer, *Chem. Commun.* **2016**, *52*, 3077–3094; d) Y. Guo, S. R. Harutyunyan, *Beilstein J. Org. Chem.* **2020**, *16*, 1006–1021.
[3] a) G. Bartoli, G. Bencivenni, R. Dalpozzo, *Chem. Soc. Rev.* **2010**, *39*, 4449–4465; b) A. Moyano, R. Rios, *Chem. Rev.* **2011**, *111*, 4703–4832; c) L. Albrecht, L. K. Ransborg, K. A. Jørgensen, *Catal. Sci. Technol.* **2012**, *2*, 1089–1098; d) B. Mondal, S. Nandi, S. C. Pan, *Eur. J. Org. Chem.* **2017**, 4666–4677; e) Y. Dudognon, J. Rodriguez, T. Constantieux, X. Bugaut, *Eur. J. Org. Chem.* **2018**, 2432–2442; f) X. Zhang, Y.-H. Chen, B. Tan, *Tetrahedron Lett.* **2018**, *59*, 473–486.
[4] a) Y.-C. Zhang, F. Jiang, F. Shi, *Acc. Chem. Res.* **2020**, *53*, 425–446; b) J. M. Alonso, M. P. Muñoz, *Eur. J. Org. Chem.* **2020**, *2020*, 7197–7213; c) F.-T. Sheng, J.-Y. Wang, W. Tan, Y.-C. Zhang, F. Shi, *Org. Chem. Front.* **2020**, *7*, 3967–3998; d) T.-Z. Li, S.-J. Liu, W. Tan, F. Shi, *Chem. Eur. J.* **2020**, *26*, 15779–15792; e) A. Cerveri, M. Bandini, *Chin. J. Chem.* **2020**, *38*, 287–294.
[5] a) D. Cheng, Y. Ishihara, B. Tan, C. F. Barbas, *ACS Catal.* **2014**, *4*, 743–762; b) G.-J. Mei, F. Shi, *Chem. Commun.* **2018**, *54*, 6607–6621; c) Z.-Y. Cao, F. Zhou, J. Zhou, *Acc. Chem. Res.* **2018**, *51*, 1443–1454; d) R. Dalpozzo, R. Mancuso, *Synthesis* **2018**, *50*, 2463–2472; e) H. Pellissier, *Synthesis* **2019**, *51*, 1311–1318.
[6] a) B. Yu, D.-Q. Yu, H.-M. Liu, *Eur. J. Med. Chem.* **2015**, *97*, 673–698; b) B. Yu, Z. Yu, P.-P. Qi, D.-Q. Yu, H.-M. Liu, *Eur. J. Med. Chem.* **2015**, *95*, 35–40; c) N. Ye, H. Chen, E. A. Wold, P.-Y. Shi, J. Zhou, *ACS Infect. Dis.* **2016**, *2*, 382–392.
[7] a) G. Bencivenni, L.-Y. Wu, A. Mazzanti, B. Giannichi, F. Pesciaioli, M.-P. Song, G. Bartoli, P. Melchiorre, *Angew. Chem. Int. Ed.* **2009**, *48*, 7200–7203; *Angew. Chem.* **2009**, *121*, 7336–7339; b) K. Jiang, Z.-J. Jia, S. Chen, L. Wu, Y.-C. Chen, *Chem. Eur. J.* **2010**, *16*, 2852–2856; c) K. Jiang, Z.-J. Jia, X. Yin, L. Wu, Y.-C. Chen, *Org. Lett.* **2010**, *12*, 2766–2769; d) Z.-J. Jia, H. Jiang, J.-L. Li, B. Gschwend, Q.-Z. Li, X. Yin, J. Grouleff, Y.-C. Chen, K. A. Jørgensen, *J. Am. Chem. Soc.* **2011**, *133*, 5053–5061; e) Y. Liu, M. Nappi, E. Arceo, S. Vera, P. Melchiorre, *J. Am. Chem. Soc.* **2011**, *133*, 15212–15218; f) C. Cassani, P. Melchiorre, *Org. Lett.* **2012**, *14*, 5590–5593; g) S. Wang, Y. Jiang, S. Wu, G. Dong, Z. Miao, W. Zhang, C. Sheng, *Org. Lett.* **2016**, *18*, 1028–1031.
[8] a) J.-A. Xiao, Q. Liu, J.-W. Ren, J. Liu, R. G. Carter, X.-Q. Chen, H. Yang, *Eur. J. Org. Chem.* **2014**, 5700–5704; b) M. Ma, Y. Zhu, Q. Sun, X. Li, J. Su, L. Zhao, Y. Zhao, S. Qiu, W. Yan, K. Wang, R. Wang, *Chem. Commun.* **2015**, *51*, 8789–8792.
[9] L. Tian, X.-Q. Hu, Y.-H. Li, P.-F. Xu, *Chem. Commun.* **2013**, *49*, 7213–7215.

[10] Q. Sun, X. Li, J. Su, L. Zhao, M. Ma, Y. Zhu, Y. Zhao, R. Zhu, W. Yan, K. Wang, R. Wang, *Adv. Synth. Catal.* **2015**, *357*, 3187–3196.
[11] a) H.-W. Zhao, Z. Yang, W. Meng, T. Tian, B. Li, X.-Q. Song, X.-Q. Chen, H.-L. Pang, *Adv. Synth. Catal.* **2015**, *357*, 2492–2502; b) Y. Lin, Y.-X. Song, D.-M. Du, *Adv. Synth. Catal.* **2019**, *361*, 1064–1070.
[12] a) F. Shi, R.-Y. Zhu, X. Liang, S.-J. Tu, *Adv. Synth. Catal.* **2013**, *355*, 2447–2458; b) C.-S. Wang, R.-Y. Zhu, J. Zheng, F. Shi, S.-J. Tu, *J. Org. Chem.* **2015**, *80*, 512–520; c) Y.-M. Wang, H.-H. Zhang, C. Li, T. Fan, F. Shi, *Chem. Commun.* **2016**, *52*, 1804–1807; d) W. Dai, X.-L. Jiang, Q. Wu, F. Shi, S.-J. Tu, *J. Org. Chem.* **2015**, *80*, 5737–5744.
[13] C. Ma, F.-T. Sheng, H.-Q. Wang, S. Deng, Y.-C. Zhang, Y. Jiao, W. Tan, F. Shi, *J. Am. Chem. Soc.* **2020**, *142*, 15686–15696.
[14] T. Peňaška, K. Ormandyová, M. Mečiarová, J. Filo, R. Šebesta, *New J. Chem.* **2017**, *41*, 5506–5512.
[15] W. Yang, D.-M. Du, *Org. Lett.* **2010**, *12*, 5450–5453.
[16] H. Jiang, M. W. Paixão, D. Monge, K. A. Jørgensen, *J. Am. Chem. Soc.* **2010**, *132*, 2775–2783.
[17] J. W. Lee, T. H. Ryu, J. S. Oh, H. Y. Bae, H. B. Jang, C. E. Song, *Chem. Commun.* **2009**, 7224–7226.
[18] B. Vakulya, S. Varga, A. Csámpai, T. Soós, *Org. Lett.* **2005**, *7*, 1967–1969.
[19] a) D. Mailhol, M. d. M. S. Duque, W. Raimondi, D. Bonne, T. Constantieux, Y. Coquerel, J. Rodriguez, *Adv. Synth. Catal.* **2012**, *354*, 3523–3532; b) Y. Zhu, J. P. Malerich, V. H. Rawal, *Angew. Chem. Int. Ed.* **2010**, *49*, 153–156; *Angew. Chem.* **2010**, *122*, 157–160.
[20] Ł. Albrecht, G. Dickmeiss, F. C. Acosta, C. Rodríguez-Escrich, R. L. Davis, K. A. Jørgensen, *J. Am. Chem. Soc.* **2012**, *134*, 2543–2546.
[21] Y. Qian, G. Ma, A. Lv, H.-L. Zhu, J. Zhao, V. H. Rawal, *Chem. Commun.* **2010**, *46*, 3004–3006.
[22] M. Rombola, C. S. Sumaria, T. D. Montgomery, V. H. Rawal, *J. Am. Chem. Soc.* **2017**, *139*, 5297–5300.
[23] M. G. Núñez, A. J. M. Farley, D. J. Dixon, *J. Am. Chem. Soc.* **2013**, *135*, 16348–16351.
[24] B. T. Cho, Y. S. Chun, *Tetrahedron: Asymmetry* **1992**, *3*, 1583–1590.
[25] Y. Sohtome, A. Tanatani, Y. Hashimoto, K. Nagasawa, *Tetrahedron Lett.* **2004**, *45*, 5589–5592.
[26] Y. Sohtome, A. Tanatani, Y. Hashimoto, K. Nagasawa, *Chem. Pharm. Bull.* **2004**, *52*, 477–480.
[27] T. Akiyama, H. Morita, J. Itoh, K. Fuchibe, *Org. Lett.* **2005**, *7*, 2583–2585.
[28] J.-D. Chai, M. Head-Gordon, *Phys. Chem. Chem. Phys.* **2008**, *10*, 6615–6620.
[29] H. S. Yu, X. He, S. L. Li, D. G. Truhlar, *Chem. Sci.* **2016**, *7*, 5032–5051.
[30] F. Weigend, R. Ahlrichs, *Phys. Chem. Chem. Phys.* **2005**, *7*, 3297–3305.
[31] J. Tomasi, B. Mennucci, R. Cammi, *Chem. Rev.* **2005**, *105*, 2999–3094.
[32] *CYLview20*, C. Y. Legault, Université de Sherbrooke, (http://www.cylview.org), **2020**.

Manuscript received: January 31, 2021
Revised manuscript received: February 3, 2021
Accepted manuscript online: February 10, 2021